produced using SIMOX. Both BESOI and SIMOX are less precise in fabricating a given film thickness of either Si or SiO_2.

Samples: The Unibond SOI wafers were obtained from SOITEC Grenoble, with an Si film thickness of 1.14μm and a buried SiO_2 layer thickness of 0.67μm. These thicknesses were chosen such that most of the output beam is diffracted towards the surface at the output grating coupler [7, 8]. The basic structure of the Unibond waveguide and the sample are shown in Fig. 1*a* and *b*, respectively. Fig. 1*a* shows the waveguide and input and output couplers, which comprise silicon rectangular gratings with a period of 0.4μm. The output gratings were designed such that the beam transmitted towards the substrate was minimised, and hence the output coupling efficiency is maximum [7]. Waveguide propagation lengths of 0.5, 1.0 and 1.5cm were used (Fig. 1*b*). The variable lengths enable us to calculate the waveguide loss accurately by averaging the output beam powers, and assuming identical coupling for each grating.

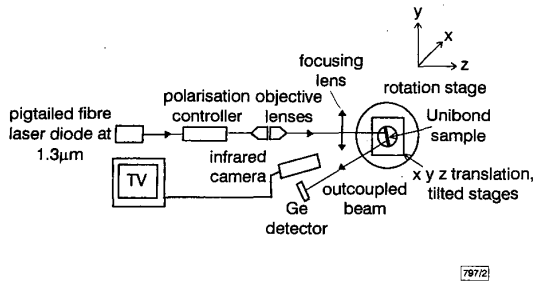

Fig. 2 *Experimental setup for measuring output beam power of Unibond sample*

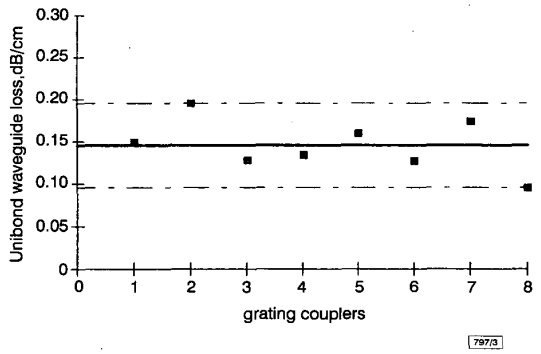

Fig. 3 *Unibond waveguide loss*

Unibond material has average loss of 0.146dB/cm ≃ 0.15dB/cm with deviation of ± 0.005dB/cm

Experiments and results: Fig. 2 shows the experimental setup for measuring the output beam from the output grating couplers. The polarisation controller was adjusted to maintain the input beam at TE polarisation, and the beam was focused into a diameter of ~300μm onto the input grating coupler. The Unibond sample was rotated, positioned and adjusted using the rotation stage, translation stage and the *x*, *y*, *z* tilted stage, respectively, until the highest power was detected by the germanium (Ge) detector. Each maximum output beam power was then recorded and the waveguide loss was then calculated taking the ratio of the output beam powers of the output couplers with reference to the difference in propagation lengths. The mean waveguide loss is 0.146dB/cm with a maximum deviation of ± 0.05dB/cm, as shown in Fig. 3. This optical loss of 0.15 ± 0.05dB/cm for planar Unibond waveguides is among the lowest loss of SOI waveguides reported and is comparable to the loss of SIMOX waveguides achieved by Rickman *et al.* [5] and Fischer *et al.* [6]. The low loss is due to several factors. First, SOI waveguide structures are strongly confining due to the high refractive index difference between the air / Si / SiO_2. Secondly, the thick SiO_2 (0.67μm) buried layer prevents high leakage of the guided beam towards the substrate [5]. Consequently, the loss of the Unibond SOI at 1.3μm is mainly due to the absorption loss of the bulk silicon. There may also be minor residual scattering at the grating surface.

Conclusion: The low loss of 0.15 ± 0.05dB/cm for Unibond waveguides is reported for the first time and it is among the lowest loss for SOI reported. This result shows that Unibond material exhibits a good quality silicon guiding layer which is comparable to that of pure silicon, allowing optical integrated circuits to be fabricated at low cost. Furthermore the manufacturing process is sufficiently flexible to allow variations in the thickness of the guiding Si layer, and the buried SiO_2 layer.

Acknowledgment: T.W. Ang is grateful for the Faculty Scholarship and ORS award from the University of Surrey. The authors are grateful to EPSRC and Bookham Technology Ltd. for financial support.

23 April 1999
Electronics Letters Online No: 19990689
DOI: 10.1049/el:19990689

T.W. Ang, G.T. Reed, A. Vonsovici (*School of Electronic Engineering, Information Technology and Mathematics, University of Surrey, Guildford, GU2 5XH, United Kingdom*)

A.G.R. Evans, P.R. Routley and M.R. Josey (*Department of Electronics and Computer Science, University of Southampton, Highfield, Southampton, SO17 1BJ, United Kingdom*)

References

1 BRUEL, M.: 'Silicon on insulator material technology', *Electron. Lett.*, 1995, **31**, (14), pp. 1201–1202

2 AUBERTON-HERVE, A.J., BRUEL, M., ASPAR, B., MALEVILLE, C., and MORICEAU, H.: 'Smart Cut: the basic fabrication process for Unibond SOI wafers', *IEICE Trans. Electron.*, 1997, **E80-C**, (3), pp. 358–363

3 MUNTEANU, D., MALEVILLE, C., CRISTOLOVEANU, S., MORICEAU, H., ASPAR, B., RAYNAUD, C., FAYNOT, O., PELLOIE, J.-L., and AUBERTON-HERVE, A.-J.: 'Detailed characteristion of Unibond material', *Microelectron. Eng.*, 1997, **36**, pp. 395–398

4 REED, G.T., LI, J.H., TANG, C.K., LU, C.L., HEMMENT, P.L.F., and RICKMAN, A.G.: 'Silicon on insulator optical waveguides formed by direct wafer bonding', *Mater. Sci. Eng.*, 1992, **B15**, pp. 156–159

5 RICKMAN, A.G., REED, G.T., WEISS, B.L., and NAMAVAR, F.: 'Low-loss planar optical waveguides fabricated in SI MOX material', *IEEE Photonics Technol. Lett.*, 1992, **4**, (6), pp. 633–635

6 FISCHER, U., ZINKE, T., KROPP, J.-R., ARNDT, F., and PETERMANN, K.: '0.1 dB/cm waveguide losses in single-mode SOI rib waveguides', *IEEE Photonics Technol. Lett.*, 1996, **8**, (5), pp. 633–635

7 ANG, T.W., REED, G.T., VONSOVICI, A., EVANS, A.G.R., ROUTLEY, P.R., BLACKBURN, T., and JOSEY, M.R.: 'Grating couplers using silicon-on-insulator'. Proc. SPIE, January 1999, **3620**, pp. 79–86

8 ANG, T.W., REED, G.T., VONSOVICI, A., EVANS, A.G.R., ROUTLEY, P.R., BLACKBURN, T., and JOSEY, M.R.: 'Silicon-on-insulator based grating couplers'. Proc. PREP '99, UMIST, Manchester, UK, 1999, pp. 108–110

Stability and bandwidth enhancement of difference frequency generation (DFG)-based wavelength conversion by pump detuning

M.H. Chou, I. Brener, K.R. Parameswaran and M.M. Fejer

The authors report on a method for enhancing the operating stability and signal bandwidth of difference-frequency-generation-based wavelength conversion by detuning the pump from the degenerate phase matching wavelength; both can be further enhanced by using nonuniform quasi-phase-matching structures.

Introduction: Difference-frequency generation (DFG), in which a pump at frequency ω_p is mixed with a signal at frequency ω_s via the second-order nonlinearity $\chi^{(2)}$ to generate an output at shifted frequency $\omega_{out} = \omega_p - \omega_s$, is an attractive method for the generation of coherent infrared radiation and manipulation of optical frequency signals. Several optical signal processing functions can be performed, such as wavelength conversion, spectral inversion, time multiplexing/demultiplexing, and clock recovery in optical networks by DFG [1, 2]. Wavelength conversion based on DFG has

been demonstrated successfully in quasi-phase-matched (QPM) waveguides [3 – 5]. Efficient wavelength conversion using cascaded second order nonlinearities ($\chi^{(2)}$:$\chi^{(2)}$) has also been demonstrated [6 – 8]. These conversion processes can accommodate a signal bandwidth of several terahertz, can simultaneously convert multiple signal channels with any signal formats, and can generate spectral inverted outputs with negligible spontaneous emission noise.

Although wavelength conversion based on DFG has a wide *signal* conversion bandwidth (~60–90nm), the *pump* bandwidth is in general narrow (~0.1nm) as will be described in the following Section. Traditionally, the pump is chosen to operate very close to the degenerate phase matching wavelength, where $\lambda_{out} = \lambda_{signal,0}$ and $\lambda_{pump,0} = \lambda_{signal,0}/2$. ($\lambda_{pump}$, λ_{signal}, and λ_{out} are pump, input signal, and converted output wavelengths, respectively; subscript 0 denotes degeneracy). However, under these circumstances, the conversion efficiency and its bandwidth will be sensitive to drifts in the device temperature or in the pump wavelength. In this Letter, we address this instability problem by detuning the pump from the degenerate phase matching wavelength. We also discuss the possibility of further enhancing the device stability and bandwidth using nonuniform QPM structures.

Theory: In nonlinear frequency conversion processes such as second harmonic generation (SHG) and DFG, the conversion efficiency in uniform devices is proportional to $\mathrm{sinc}^2(\Delta\beta L/2)$, where $\Delta\beta L$ is the phase mismatch between the interacting waves for a given QPM grating. We can expand the phase mismatch $\Delta\beta L$ in a Taylor series as a function of an arbitrary parameter ξ (such as λ_{signal}, λ_{pump} or temperature):

$$\Delta\beta L(\xi) = \Delta\beta L(\xi_0) + (\xi-\xi_0)\frac{d}{d\xi}\Delta\beta L(\xi_0) + \frac{(\xi-\xi_0)^2}{2}\frac{d^2}{d\xi^2}\Delta\beta L(\xi_0) + \cdots \quad (1)$$

For near-degenerate DFG ($\lambda_{out} \simeq \lambda_{signal} \simeq 2\lambda_{pump}$), the first derivative of phase mismatch with respect to the signal wavelength is equal to zero, due to the signal and output wavelengths moving in opposite directions with signal tuning at fixed pump wavelength. Thus, the phase mismatch depends only on the second and higher order derivatives, resulting in a wide signal bandwidth. However, the first derivative of the phase mismatch with respect to the pump wavelength at a fixed signal wavelength is not zero, because no signal and output wavelength tune in the same direction. This results in a strong dependence on the pump wavelength, demanding good pump wavelength and temperature stability for practical device operation.

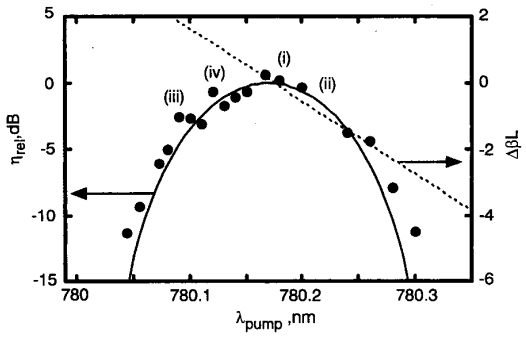

Fig. 1 *Relative conversion efficiency (η_{rel}) and calculated phase mismatch ($\Delta\beta L$) against pump wavelength (λ_{pump})*

Signal is fixed at ~$\lambda_{signal,0}$, η_{rel} = –3dB at $\Delta\beta L = \pm 0.443\pi$
Points (i)–(iv) correspond to the values of λ_{pump} used in Fig. 2

To efficiently access the wide signal conversion bandwidth, it is sub-optimal to pump at the degenerate wavelength $\lambda_{pump,0}$. Instead, the pump wavelength should be chosen to be slightly shorter than degeneracy to achieve global optimisation. To illustrate this, we performed wavelength conversion using a DFG-based device under different pump conditions. The device was fabricated by annealed proton exchange in periodically poled $LiNbO_3$. It includes integrated waveguide structures for efficient mode coupling [5] and a 40mm-long wavelength conversion section with a QPM grating period of 15μm.

Experiment: Fig. 1 shows the relative conversion efficiency (η_{rel}) and calculated phase mismatch ($\Delta\beta L$) against λ_{pump}, with λ_{signal} fixed close to $\lambda_{signal,0}$ = 1560.34nm. The efficiencies η_{rel} are normalised to the peak conversion efficiency, which is ~–4dB with ~90mW of pump power coupled into the waveguides. Using a pump fixed at $\lambda_{pump,0}$, we measured η_{rel} against λ_{signal}, as shown in Fig. 2(i). The 3dB bandwidth of this device is ~56nm. η_{rel} is 0dB at $\lambda_{signal,0}$ (where $\Delta\beta L = 0$) and decreases slowly when the signal moves away from this point.

Fig. 2(ii) and (iii) show the relative conversion efficiency η_{rel} and phase mismatch $\Delta\beta L$ with the pump at wavelengths of $\lambda_{pump,0} \pm 0.065$nm. For the higher wavelength pump, η_{rel} is –3dB at $\lambda_{signal,0}$ and is reduced significantly at other signal wavelengths. This indicates the instability caused by operating the pump at $\lambda_{pump,0}$, since small pump wavelength up-drift will result in a significant drop in efficiency. For the shorter pump wavelength, η_{rel} is –3dB for $\lambda_{signal,0}$ but increases when the signal moves away from this point. Under this condition, there are two phase matching wavelengths (where $\Delta\beta L = 0$) such that the 3dB bandwidth is 78nm, which is 22nm wider than that when pumped at $\lambda_{pump,0}$. This suggests that the pump wavelength should be chosen in between the conditions of (i) and (iii), allowing for both upward and downward drift of pump wavelength and/or temperature, as shown in Fig. 2(iv).

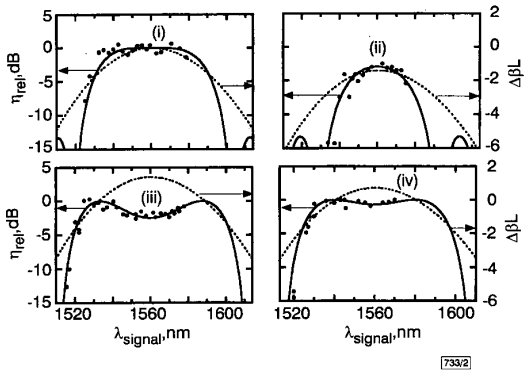

Fig. 2 *Conversion efficiency (η_{rel}) and calculated phase mismatch ($\Delta\beta L$) against input signal wavelengths (λ_{signal}) for pump at wavelength as indicated in Fig. 1*

(i) 780.17nm
(ii) 780.105nm
(iii) 780.235nm
(iv) 780.138nm
● measured results
——— theoretical fit
– – – – calculated $\Delta\beta L$

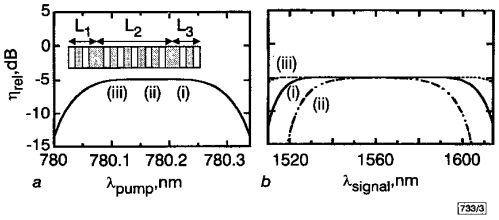

Fig. 3 *η_{rel} against λ_{pump} for QPM structure with phase-reversal gratings and η_{rel} against λ_{signal} for three different pump wavelengths*

a η_{rel} against λ_{pump}
b η_{rel} against λ_{signal}
Inset: schematic diagram of QPM structures
Pump wavelengths:
(i) 780.17nm
(ii) 780.105nm
(iii) 780.235nm

Nonuniform grating and cascaded second order nonlinearity: The device stability can be further optimised by using nonuniform QPM gratings. It has been shown that QPM gratings with dephasing domains enhance the SHG bandwidth [9]. In the follow-

ing, we theoretically investigate nonuniform QPM gratings, as shown in the inset of Fig. 3(i), for DFG wavelength conversion. The structure used here consists of three segments with length of L_1, L_2, L_3 where $L_1 = L_3$, device length ($L = L_1 + L_2 + L_3$) is 40mm, and $L_1/L = 0.107$. Fig. 3(i) shows the calculated η_{rel} against λ_{pump} for a QPM structure with phase-reversal gratings and the same device parameters as before. Fig. 3(ii) shows the η_{rel} against λ_{signal} for different pump wavelengths. This QPM structure broadens the pump and signal bandwidth (signal banwidth > 100nm, but with some efficiency reduction). To efficiently use this nonuniform QPM grating, it is again necessary to operate the pump at an off-degenerate wavelength.

1.5μm wavelength conversion based on $\chi^{(2)}$:$\chi^{(2)}$ allows for the use of a pump within the 1.5μm band. The frequency mixing process involves the cascading of SHG and DFG, which can be implemented using either co-propagating or counter-propagating pump and signal beams [6 – 8]. The method described above can be immediately applied to the counter-propagating scheme, in which the 1.5μm pump is frequency doubled by SHG, then reflected back into waveguides by a dichroic mirror to mix with signals by DFG. For the co-propagating scheme where SHG and DFG occur simultaneously, further optimisation of nonuniform QPM gratings will be required.

Conclusion: In summary, we have used pump detuning to address instability issues in DFG-based wavelength conversion. We also describe further enhancement of device stability and bandwidth by using a nonuniform QPM structure. These approaches can also be applied to wavelength conversion based on cascaded second order nonlinearities.

Acknowledgments: This search was sponsored by JSEP, by DARPA through the OMC, and by Lucent Technologies. We also thank Crystal Technology for donating $LiNbO_3$ substrates.

21 April 1999
Electronics Letters Online No: 19990678
DOI: 10.1049/el:19990678

M.H. Chou, K.R. Parameswaran and M.M. Fejer (*E.L. Ginzton Laboratory, Stanford University, Stanford, CA 94305-4085, USA*)

E-mail: choumh@lelend.stanford.edu

I. Brener (*Bell Laboratories, Lucent Technologies, 700 Mountain Avenue, Murray Hill, NJ 07974, USA*)

References

1 YOO, S.J.B.: 'Wavelength conversion technologies for WDM network applications', *J. Lightwave Technol.*, 1996, **LT-14**, pp. 955–966
2 KAWANISHI, S.: 'Ultrahigh-speed optical time-division-multiplexed transmission technology based on optical signal processing', *J. Quantum Electron.*, 1998, **QE-34**, pp. 2064–2079
3 YOO, S.J.B., KOZA, M.A., CANEAU, C., and BHAT, R.: 'Simultaneous wavelength conversion of 2.5-Gbit/s and 10-Gbit/s signal channels by difference-frequency generation in an AlGaAs waveguide'. Conf. on Optical Fiber Communications, Vol. 2 of 1998 OSA Tech. Dig. Ser., Paper WB5
4 XU, C.Q., OKAYAMA, H., and KAWAHARA, M.: '1.5μm band efficient broadband wavelength conversion by difference frequency generation in a periodically domain-inverted $LiNbO_3$ channel waveguide', *Appl. Phys. Lett.*, 1993, **63**, pp. 3559–3561
5 CHOU, M.H., HAUDEN, J., ARBORE, M.A., and FEJER, M.M.: '1.5μm-band wavelength conversion based on difference-frequency generation in $LiNbO_3$ waveguides with integrated coupling structures', *Opt. Lett.*, 1998, **23**, pp. 1004–1006
6 GALLO, K., ASSANTO, G., and STEGEMAN, G.: 'Efficient wavelength shifting over the erbium amplifier bandwidth via cascaded second order processes in lithium niobate waveguides', *Appl. Phys. Lett.*, 1997, **71**, pp. 1020–1022
7 TREVINO-PALACIOS, C.G., STEGEMAN, G.I., DE BALDI, P., and MICHELI, M.P.: 'Wavelength shifting using cascaded second-order processes for WDM applications at 1.55μm', *Electron. Lett.*, 1998, **34**, pp. 2157–2158
8 BRENER, I., CHOU, M.H., and FEJER, M.M.: 'Efficient wideband wavelength conversion using cascaded second-order nonlinearities in $LiNbO_3$ waveguides'. Conf. on Optical Fiber Communications, 1999, Paper FB6
9 MIZUUCHI, K., and YAMAMOTO, K.: 'Waveguide second-harmonic generation device with broadened flat quasi-phase-matching response by use of a grating structure with located phase shifts', *Opt. Lett.*, 1998, **23**, pp. 1880–1882

90mW 660nm distributed feedback lasers

M. Hagberg, B. Pezeshki, S. Zou, M. Zelinski and E. Kolev

High efficiency single spatial and spectral mode, 662nm wavelength distributed feedback lasers have been fabricated from a GaInP/AlInP laser structure. Output powers of up to 90mW at room temperature were achieved without any spectral mode jumps. These devices should be useful for short and/or visible wavelength applications that require spectral mode stability, such as spectroscopy, interferometry, and high-density optical storage.

Visible wavelength single spatial mode Fabry-Perot diode lasers are produced in large quantities for a variety of uses such as optical storage and pointing. For these applications, the requirements on spectral width and stability are relatively relaxed. Other applications for visible lasers require low modal intensity noise and narrow spectral width, where Fabry-Perot diodes are inappropriate. Examples include spectroscopy, interferometry, and novel schemes for high-density optical storage.

Grating stabilised lasers at 1.3 and 1.55μm have been developed and used extensively in the InGaAsP material system for fibre-optic communication applications. The lack of a comparable driving force has limited the efforts of developing DFB or DBR lasers in the harder-to-master GaInP/AlInP system. The progress of buried grating technologies in wider bandgap structures, that contain high levels of aluminium, has previously been problematic due to regrowth difficulties.

DFB lasers, lasing in the 630–690nm band, have previously been demonstrated CW at low temperatures, pulsed at room temperature, in broad area structures, and CW at room temperature [1 – 5]. The power from visible narrow stripe DFB lasers has since then been boosted to 40mW using improved regrowth techniques [6]. For a novel broad area cavity design, the α-DFB laser, an impressive 400mW single spatial and spectral mode at 660nm has been reported at the cost of lower wallplug efficiency [7]. High power is required or convenient for applications such as Raman spectroscopy and read/write optical storage. In this work we demonstrate high performance 90mW DFB lasers at 660nm wavelength. It is the highest reported CW power from a narrow waveguide single spatial and spectral mode device emitting in the visible wavelength range.

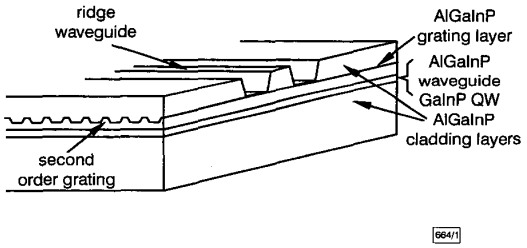

Fig. 1 *DFB laser schematic diagram*

Gain is provided by strained GaInP quantum wells placed in an AlGaInP waveguide
Buried grating close to waveguide provides wavelength selective feedback

The epitaxial structure was grown in a low pressure MOCVD reactor on an *n*-doped GaAs substrate. Fig. 1 shows a schematic diagram of the epitaxial and waveguide design. The initial growth includes an AlInP lower cladding layer, an AlGaInP waveguide with a strained GaInP QW, the lower part of an AlInP upper cladding layer, and an AlGaInP grating layer. The waveguide is designed for single spatial mode operation and the position relative to the grating layer was chosen such that the optical mode overlap with the grating layer is sufficient for feedback.

A grating was patterned in thin photoresist using an HeCd laser in a setup for holographic exposure and the pattern was subsequently transferred ~30nm into the grating layer. The grating pitch was 206nm corresponding to in-plane reflection through second order diffraction. Although in-plane reflection through first order diffraction would have been preferred in order to avoid sur-